Macromolecules **2002,** *35,* 4960−4967

Synthesis, Characterization, and Properties of ABA Type Triblock Copolymer Brushes of Styrene and Methyl Acrylate Prepared by Atom Transfer Radical Polymerization

Stephen G. Boyes, William J. Brittain,* Xin Weng, and Stephen Z. D. Cheng

Department of Polymer Science, The University of Akron, Akron, Ohio 44325-3909

Received January 22, 2002; Revised Manuscript Received April 19, 2002

ABSTRACT: A tethered triblock copolymer has been synthesized by sequential monomer addition to a self-assembled monolayer of (11-(2-bromo-2-methyl)propionyloxy)undecyltrichlorosilane. Si/SiO_2//polystyrene-*b*-poly(methyl acrylate)-*b*-polystyrene (PS-*b*-PMA-*b*-PS) and Si/SiO_2//PMA-*b*-PS-*b*-PMA were prepared by the "grafting from" method using atom transfer radical polymerization. The resulting triblock brushes were characterized by ATR−FTIR, water contact angles, ellipsometry, X-ray photoelectron spectroscopy (XPS), and atomic force microscopy (AFM). Free polymer formed during the brush formation was characterized by gel permeation chromatography. Treatment of the triblock brushes with block-selective solvents caused reversible changes in the water contact angles and AFM. AFM analysis revealed a patterned nanomorphology when the brush was treated with a good solvent for the mid-block. We have interpreted this nanomorphology in terms of a folded brush structure where the two end blocks aggregate and force the mid-block to the air interface. XPS and water contact angle observations are consistent with this interpretation.

Introduction

Polymer brushes refer to an assembly of polymer chains which are tethered by one end to a surface or interface.[1,2] Tethering of the chains in close proximity to each other forces the chains to stretch away from the surface to avoid overlapping. Polymer brushes have recently attracted considerable attention, and there have been numerous studies to examine their structure and novel properties.[3−9] As such, polymer brushes have found application in a broad range of fields, including colloid stabilization,[10] tailoring surface properties, and "chemical gates".[5] Polymer brushes are typically synthesized by two different methods: physisorption and covalent attachment. Polymer physisorption normally involves absorption of block copolymers onto a substrate, where one block interacts strongly with the surface and the other block forms the brush layer.[11] The disadvantages of physisorption include thermal and solvolytic instabilities due to the noncovalent nature of the grafting, poor control over polymer chain density, and complications in synthesis of suitable block copolymers. Tethering of the polymer chains to the surface is one way to surmount some of these disadvantages.

Covalent attachment of polymer brushes can be achieved by either "grafting to" or "grafting from" techniques. The "grafting to" technique involves tethering preformed end-functionalized polymer chains to a suitable substrate under appropriate conditions.[12] This technique often leads to low grafting density and low film thickness, as the polymer molecules must diffuse through the existing polymer film to reach the reactive sites on the surface. The steric hindrance for surface attachment increases as the tethered polymer film thickness increases. To overcome this problem, the "grafting from" approach can be used and has generally become the most attractive way to prepare thick, covalently tethered polymer brushes with a high grafting density.[13] The "grafting from" technique involves the immobilizing of initiators onto the substrate followed by in situ surface-initiated polymerization to generate the tethered polymer brush. Surface immobilized initiators can be generated by either treating the substrate with plasma or glow discharge in the presence of a gas[14] or forming initiator containing self-assembled monolayers (SAMs) on the substrates.[15,16] As the chains are growing from the surface, the only limit to propagation is diffusion of monomer to the chain ends, thus resulting in thick tethered polymer brushes with high grafting density.

Recent advances in polymer synthesis techniques have given rise to the importance of "living" free radical polymerization, as it provides a number of advantages over traditional free radical techniques.[17] The main advantages that a "living" free radical system provides for polymer brush synthesis are control over the brush thickness, via control of molecular weight and narrow polydispersities, and the ability to prepare block copolymers by the sequential activation of the dormant chain end in the presence of different monomers.[18,19] Probably the most common "living" radical technique to produce polymer brushes is atom transfer radical polymerization (ATRP).[19−23] In earlier work, we observed the formation of unusual nanomorphologies for tethered diblock copolymers that were treated with block-selective solvents.[7,8] Treatment of Si/SiO2//PS-*b*-PMMA with cyclohexane (a selective solvent for the PS block) resulted in the formation of a patterned surface that was interpreted in terms of pinned micelles. Motivated by this earlier work, we decided to synthesize and characterize an ABA triblock copolymer brush. Our goal was to determine whether the compatibility of the two end blocks would create a similar nanomorphology. In this report we detail the use of ATRP to synthesize ABA type triblock copolymer brushes of styrene and methyl acrylate and characterization of the resulting tethered brush systems.

10.1021/ma020109m CCC: \$22.00

Experimental Section

Materials. Methyl acrylate (MA, Aldrich, 99%) and styrene (S, Aldrich, 99%) were passed through a column of activated basic alumina (Aldrich, ~150 mesh) and purged with high-purity nitrogen for 1 h prior to use. (11-(2-Bromo-2-methyl)-propionyloxy)undecyltrichlorosilane was synthesized as described in the literature.[19] CuBr (Aldrich, 98%) was purified as described in the literature.[24] *N*,*N*,*N*′,*N*′,*N*″-Pentamethyldiethylenetriamine (PMDETA, Aldrich, 99%), ethyl 2-bromoisobutyrate (Br-iB, Aldrich, 98%), anhydrous anisole (Aldrich), dichloromethane, acetone, and ethanol (EtOH) were used as received. Silicon ATR crystals (25 × 5 × 1 mm) were obtained from Harrick Scientific. Silicon wafers were purchased from Semiconductor Processing, Inc., and cut into 25 × 10 mm pieces using a diamond-tipped glass cutter. All other reagents were purchased from either Aldrich or Fisher and used as received.

Substrate Preparation. ATR crystals and silicon wafers were cleaned by treatment with freshly prepared “piranha” solution (70/30, v/v, concentrated H_2SO_4/30% aqueous H_2O_2) at 90 °C overnight and were then rinsed with distilled water and dried with a stream of clean air. It should be noted that the “piranha” solution is extremely reactive and should be handled with great care.

General Procedure for Deposition of Surface Bound Initiator. Into a dried round-bottom flask was placed a freshly cleaned silicon wafer and ATR crystal. The flask was sealed using a septum and flushed with high-purity nitrogen for 30 min. Dry toluene (10 mL) and a 25 vol % solution of the trichlorosilane initiator in toluene (0.2 mL) were added to the flask via syringe, and the flask was heated at 60 °C for 4 h under an atmosphere of nitrogen. The silicon wafer and ATR crystal were then removed, sequentially washed with toluene, EtOH, and CH_2Cl_2, and then dried in a stream of air.

Typical Procedure for Surface ATRP from a Flat Silicon Substrate. An ATR crystal and silicon wafer were placed in a 100 mL Schlenk flask and sealed with a rubber septum. The flask was degassed and back-filled with nitrogen three times and left under nitrogen. CuBr, anisole, and monomer were added to a separate 100 mL Schlenk flask with a magnetic stirrer bar, sealed with a rubber septum, and degassed by purging with nitrogen for 1 h. PMDETA was added to the mixture via syringe, and the solution was stirred at 90 °C until it became homogeneous (approximately 15 min). The solution was then transferred to the flask containing the ATR crystal and silicon wafer via cannula, followed by the addition of free initiator, Br-iB, via syringe. The final concentrations were as follows: $[S]_0 = 3.9$ M, $[PMDETA]_0 = 25$ mM, $[CuBr]_0 = 12$ mM and $[Br\text{-}iB]_0 = 10$ mM or $[MA]_0 = 3.7$ M, $[PMDETA]_0 = 25$ mM, $[CuBr]_0 = 12$ mM and $[Br\text{-}iB]_0 = 10$ mM. The polymerization was allowed to proceed at 90 °C for 24 h, after which the ATR crystal and silicon wafer were removed and rinsed with CH_2Cl_2. To remove untethered polymer, the ATR crystal and silicon wafer were placed in a Soxhlet extractor and extracted with CH_2Cl_2 for 24 h. Free polymer from the polymerization solution was isolated by first evaporating residual monomer and solvent, dissolving in THF, and then passing the THF/polymer solution through a short column of activated basic alumina to remove any residual catalyst.

Block Copolymerizations. Block copolymerizations were performed in the same manner as the typical ATRP procedures for styrene and MA. The order of addition was governed by the use of ATR crystals and silicon wafers containing the initial polymer brushes. For example, the Si/SiO_2//PS-*b*-PMA-*b*-PS brush was produced by performing the following typical ATRP procedures in the order styrene, methyl acrylate, and styrene. After each polymerization the ATR crystal and silicon wafer were cleaned and extracted to remove any untethered polymer before proceeding to the next polymerization.

Treatment of Si/SiO_2//PS-*b*-PMA-*b*-PS Brushes with Acetone. The sample was first immersed in CH_2Cl_2 at 40 °C for 30 min to recover the original state. The Si/SiO_2//PS-*b*-PMA-*b*-PS brush was then immersed in 20 mL of acetone at 40 °C for 30 min. The sample was then removed from the solvent and dried with a stream of clean air followed by characterization with tensiometry, XPS, and AFM.

Treatment of Si/SiO_2//PMA-*b*-PS-*b*-PMA Brushes with Cyclohexane. The sample was first immersed in CH_2Cl_2 at 40 °C for 30 min to recover the original state. The Si/SiO_2//PMA-*b*-PS-*b*-PMA brush was then immersed in 20 mL of cyclohexane at 40 °C for 30 min. The sample was then removed from the solvent and dried with a stream of clean air followed by characterization with tensiometry, XPS, and AFM.

Characterization Methods. FTIR-ATR spectra were recorded using a Nicolet System 730 spectrometer using a modified 4XF beam condenser (Harrick Scientific). Spectra were recorded at 2 cm^{-1} resolution, and 500 scans were collected. Contact angles were determined using a Rame Hart NRL-100 contact angle goniometer equipped with an environmental chamber and tilting base mounted on a vibrationless table (Newport Corp.). Advancing and receding values were determined using the tilting stage method. Drop volumes were 10 μL. Ellipsometric measurements were performed on a Gaertner model L116C ellipsometer with He−Ne laser ($\lambda = 632.8$ nm) and a fixed angle of incidence of 70°. For the calculation of the layer thickness, refractive indecies of $n = 1.455$ (for silicon oxide),[25] $n = 1.444$ (for the initiator layer), $n = 1.5894$ (for PS),[25] and $n = 1.480$ (for PMA)[25] were used. AFM was performed using a Multimode scanning probe microscope (Digital Instruments) in tapping mode with a silicon tip. The AFM images were obtained at room temperature in air. Molecular weight distributions were determined by size-exclusion chromatography (SEC) using a Waters 501 pump, Waters HR4 and HR2 styragel columns, a Waters 410 differential refractometer, and a Viscotek T60A dual light scattering and viscosity detector. Molecular weights were determined using Universal calibration. X-ray photoelectron spectroscopy (XPS) was performed on a Perkin-Elmer instrument using Al Kα radiation at The MATNET Surface Analysis Centre at Case Western Reserve University. The takeoff angle was 45°, and the incidence angle of X-rays was 45° with respect to surface normal, making the X-ray to electron angle 90°. Survey spectra were taken after the sample was treated with different solvents.

Results and Discussion

Synthesis and Characterization of Tethered Triblock Copolymer Brushes on Flat Silicate Substrates. The synthesis of tethered triblock copolymer brushes of styrene and methyl acrylate on flat silicate substrates via a “grafting from” approach is illustrated in Scheme 1. Scheme 1 outlines the preparation of a Si/SiO_2//PS-*b*-PMA-*b*-PS triblock copolymer. A similar approach was used to produce the Si/SiO_2//PMA-*b*-PS-*b*-PMA triblock copolymer. Preparation of the triblock copolymers involves immobilization of a bromo-isobutyrate ATRP initiator onto the silicate substrate by a self-assembly technique. The bromo-isobutyrate ATRP initiator used was (11-(2-bromo-2-methyl)propionyloxy)-undecyltrichlorosilane and was synthesized as described in the literature.[19] This initiator has been previously used to produce polymer brushes of both methyl methacrylate[18] and styrene.[19] The ATR−FTIR spectrum of the immobilized initiator (Figure 1a) shows peaks at 2925 and 2853 cm^{-1}, which are assigned to the C−H stretching and CH_2 stretching vibration, respectively, and 1736 cm^{-1}, which is assigned to the carbonyl stretching vibration of the ester group.

The detailed experimental conditions for the ATRP reactions to produce the tethered triblock copolymer brushes are described in the Experimental Section. Table 1 outlines the properties of the obtained polymers. The catalyst system used was CuBr/PMDETA, and the polymerizations were carried out at 90 °C for 24 h. Free

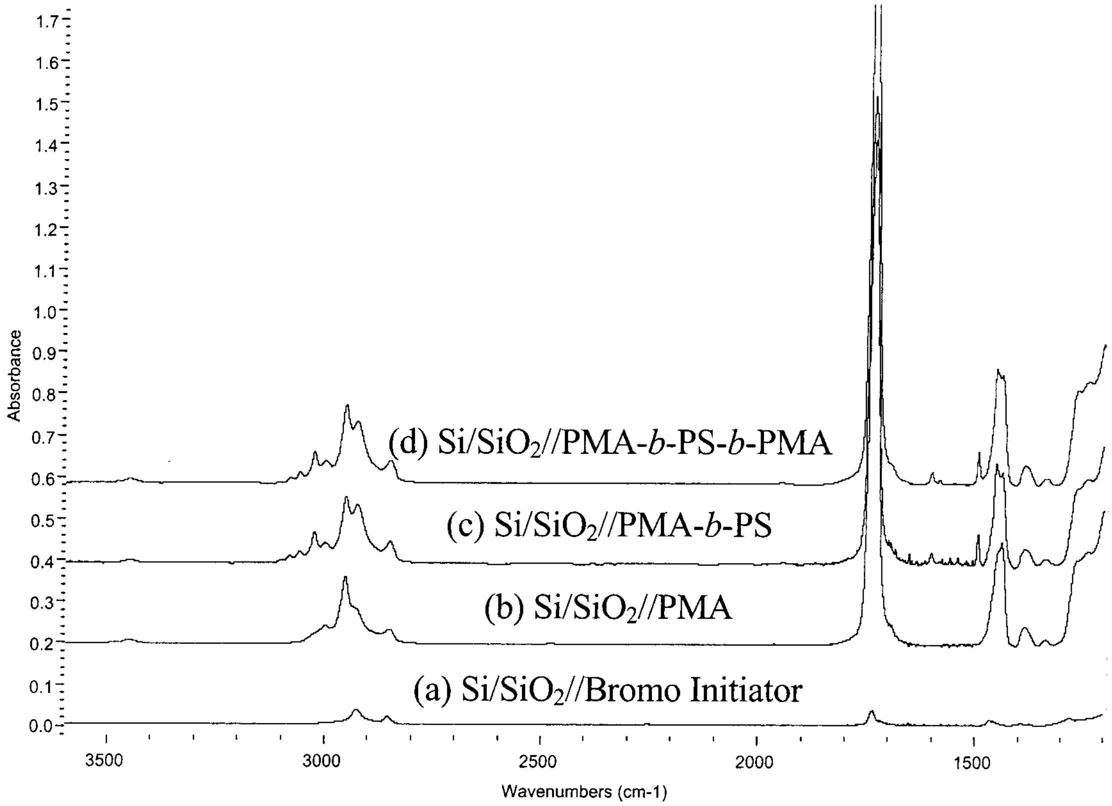

Figure 1. ATR–FTIR spectra of (a) Si/SiO_2//bromo-isobutyrate initiator, (b) Si/SiO_2//PMA (tethered PMA brush), (c) Si/SiO_2//PMA-*b*-PS, and (d) Si/SiO_2//PMA-*b*-PS-*b*-PMA.

Scheme 1. Synthesis of PS-*b*-PMA-*b*-PS Brush on a Silicon Substrate

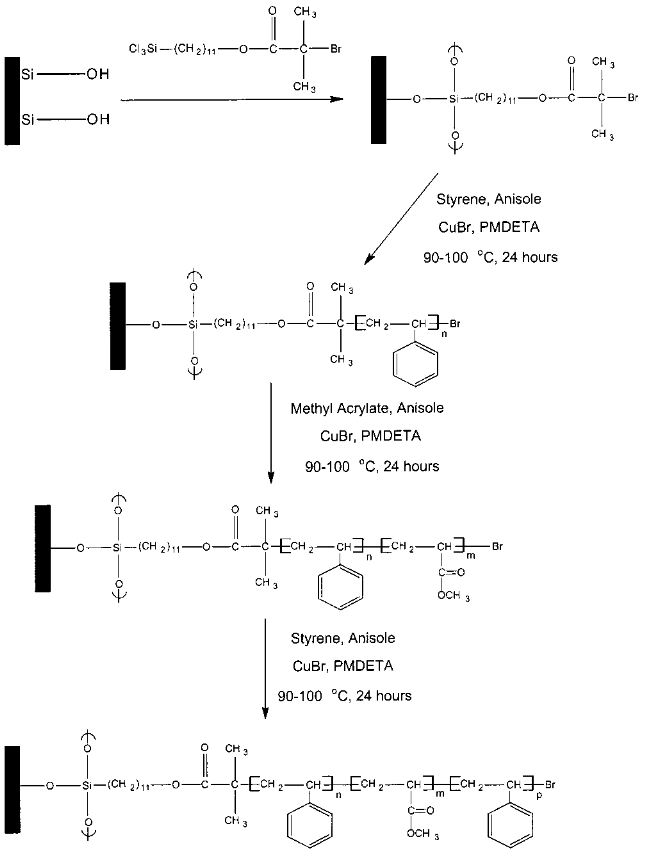

initiator, ethyl 2-bromoisobutyrate, was added to the polymerization. It has been reported that free initiator is required to provide a sufficiently high concentration of deactivator, which is necessary for controlled polymerizations on the surface.[18] Without polymerization in solution, the concentration of the deactivating copper(II) species is insufficient and control is not obtained. The other advantage to using free initiator is that the free polymer in solution has been shown to have a linear correlation with film thickness.[18,19] Therefore, since the amount of polymer on the silicon wafer is too small to degraft and analyze, the polymer in solution may provide a indication of the properties of the polymer on the surface.[18] Samples were extracted for 24 h in CH_2Cl_2 to remove any untethered polymer from the substrates.

The values in Table 1 outline the properties for each of the layers of the triblock copolymer brushes produced. Each of the values shown is representative of the outer layer only. The experimental molecular weight values shown in Table 1 are from the free polymer in solution, and the calculated molecular weights are calculated from the overall conversion of monomer, which was determined by gravimetry. The good agreement between the experimental and calculated molecular weights, and the narrow molecular weight distributions, indicate that the solution polymerization in each case is a controlled polymerization. Previous reports have shown that there is generally good agreement between the molecular weight values of the free polymer and the tethered polymer chains.[26,27] These studies also show that in the majority of cases the PDI of the tethered chains is slightly broader when compared to the PDI of the free polymer. This is explained by radical–radical termination reactions between the tethered polymer chains.[27] Thickness measurements in Table 1 suggest that the reinitiation efficiency decreased for the outer block in each case, as the thickness of the outer block was significantly lower than the first layer even though the

Table 1. Physical Properties of Triblock Copolymer Brushes

	water contact angle[a] (deg)			mol wt (M_n)		
layer	θ_a	θ_r	thickness[b] (nm)	calcd[c]	expt[d]	PDI
PS	97	87	20	13.2×10^3	10.5×10^3	1.10
PS-*b*-PMA	73	63	18	17.9×10^3	17.2×10^3	1.23
PS-*b*-PMA-*b*-PS	88	70	3	21.7×10^3	18.6×10^3	1.07
PMA	72	59	20	15.2×10^3	13.6×10^3	1.50
PMA-*b*-PS	87	72	23	21.8×10^3	18.7×10^3	1.08
PMA-*b*-PS-*b*-PMA	73	58	15	18.4×10^3	15.5×10^3	1.23

[a] The standard deviation of contact angles was <2°. [b] Thickness determined by ellipsometry. [c] Calculated using the conversion determined from the free polymer. [d] Experimental molecular weight of the free polymer.

same experimental conditions were used. This is believed to be due to radical−radical termination in preparation of the previous layers, resulting in tethered chains that are unable to reinitiate. The contact angle for both the outer PS layer in the Si/SiO$_2$//PS-*b*-PMA-*b*-PS triblock brush and the middle PS layer in the Si/SiO$_2$//PMA-*b*-PS-*b*-PMA triblock brush were significantly lower than the characteristic contact angle for PS ($\theta_a \approx 99°$).[28] This is believed to be due to the presence of PMA at the surface in each of these cases.

The vast majority of literature on tethered polymer brushes is for homopolymer or diblock copolymer brushes; to the best of our knowledge, there have been no previous reports on tethered triblock copolymer brushes. The preparation of triblock copolymers in solution using ATRP techniques has been previously reported.[29,30] Davis and Matyjaszewski[30] reported on the synthesis of both asymmetric and symmetric ABA triblock copolymers of styrene and *tert*-butyl acrylate using the CuBr/PMDETA catalyst system in conjunction with an alkyl bromide initiator. Symmetric triblock copolymers are formed by the use of a difunctional initiator to produce the middle block followed by polymerization of the resultant difunctional macroinitiator to produce the triblock copolymer. Asymmetric triblock copolymers are produced by sequential polymerization of the monomers starting from a monofunctional initiator. The main advantages in using a difunctional initiator to produce the triblock copolymer are that only two polymerization steps are required. This should reduce the overall amounts of radical−radical termination by reducing the number of polymerizations required and also enable production of symmetric triblock copolymers. However, as the ATRP initiator used in this work is tethered to the silicon substrate at one end, it is very difficult to produce tethered symmetric triblock copolymers brushes; thus, sequential polymerization was used to create asymmetric triblocks.

The ATR−FTIR spectra for the tethered Si/SiO$_2$//PMA-*b*-PS-*b*-PMA polymer brush, formed by the alternating polymerization of MA and styrene monomers, are shown in Figure 1. The ATR−FTIR spectrum of the first PMA layer is shown in Figure 1b. The PMA spectrum shows characteristic peaks at 2924 and 2852 cm^{-1} for asymmetric CH$_2$ stretching and symmetric CH$_2$ stretching, respectively, and also at 1734 cm^{-1} for the C═O stretch. After reaction of the initial PMA layer with styrene, the ATR−FTIR spectrum (Figure 1c) showed the presence of peaks at 3026, 3060, and 3082 cm^{-1}, all attributed to aromatic C−H stretching vibrations. Further addition of PMA to form the triblock copolymer brush is confirmed by an increase in the intensity of the CH$_2$ peaks (Figure 1d). Similar results and peak assignments were seen in the ATR−FTIR spectra for the Si/SiO$_2$//PS-*b*-PMA-*b*-PS triblock copolymer brush (Figure 2a−d).

Table 2. Contact Angles[a] (deg) for Solvent Treatment of Triblock Copolymer Brushes

	PS-*b*-PMA-*b*-PS		PMA-*b*-PS-*b*-PMA	
solvent	θ_a	θ_r	θ_a	θ_r
first CH$_2$Cl$_2$	91	72	69	52
first acetone/cyclohexane[b]	74	56	90	72
second CH$_2$Cl$_2$	94	75	70	52
second acetone/cyclohexane[b]	72	59	92	72

[a] The standard deviation of contact angles was <2°. [b] PS-*b*-PMA-*b*-PS brush was treated with acetone and PMA-*b*-PS-*b*-PMA brush as treated with cyclohexane.

Solvent Treatment of Triblock Copolymer Brushes. The influence of solvent on the surface properties of diblock copolymer brushes has been previously reported.[7] Each of the triblock copolymer brushes was treated with a solvent that was a good solvent for the middle block but a nonsolvent for the tethered and outer blocks. For the Si/SiO$_2$//PS-*b*-PMA-*b*-PS brush the solvent chosen was acetone, and for the Si/SiO$_2$//PMA-*b*-PS-*b*-PMA brush the solvent was cyclohexane. After treatment with solvent the water contact angle of the brush was measured, and then the process was repeated; these values are listed in Table 2. Contact angles are very sensitive to the topmost surface composition changes, with a sensing depth of approximately 0.5−1 nm,[31] with many factors such as surface roughness and chemical heterogeneity having significant effects on contact angle values. The contact angles for the Si/SiO$_2$//PS-*b*-PMA-*b*-PS brush indicate that after the initial treatment with CH$_2$Cl$_2$, which is a good solvent for all blocks, the majority of the polymer localized at the air interface is PS. As mentioned previously, the deviation in this value from the characteristic water contact angle for PS is believed to be due to low initiation efficiency of the middle PMA block, resulting in a thin outer PS layer and the presence of small amounts of PMA at the air interface. After treatment of the Si/SiO$_2$//PS-*b*-PMA-*b*-PS brush with acetone the advancing and receding contact angles decreased to 74° and 56°, respectively. These values are almost identical to the characteristic values for PMA. Subsequent treatment with CH$_2$Cl$_2$ changed the contact angles back to their original values. The switching of water contact angles was reversible for many cycles of alternating solvent treatment.

A similar response was seen for the Si/SiO$_2$//PMA-*b*-PS-*b*-PMA brush when it was treated with cyclohexane, although in this case treatment with CH$_2$Cl$_2$ resulted in the characteristic contact angle for PMA and treatment with cyclohexane resulted in close to the characteristic contact angle for PS. The deviation from the characteristic contact angle of PS in this case is believed to be due to the size of the triblock brush. As each of the blocks is approximately 20 nm long, rearrangement

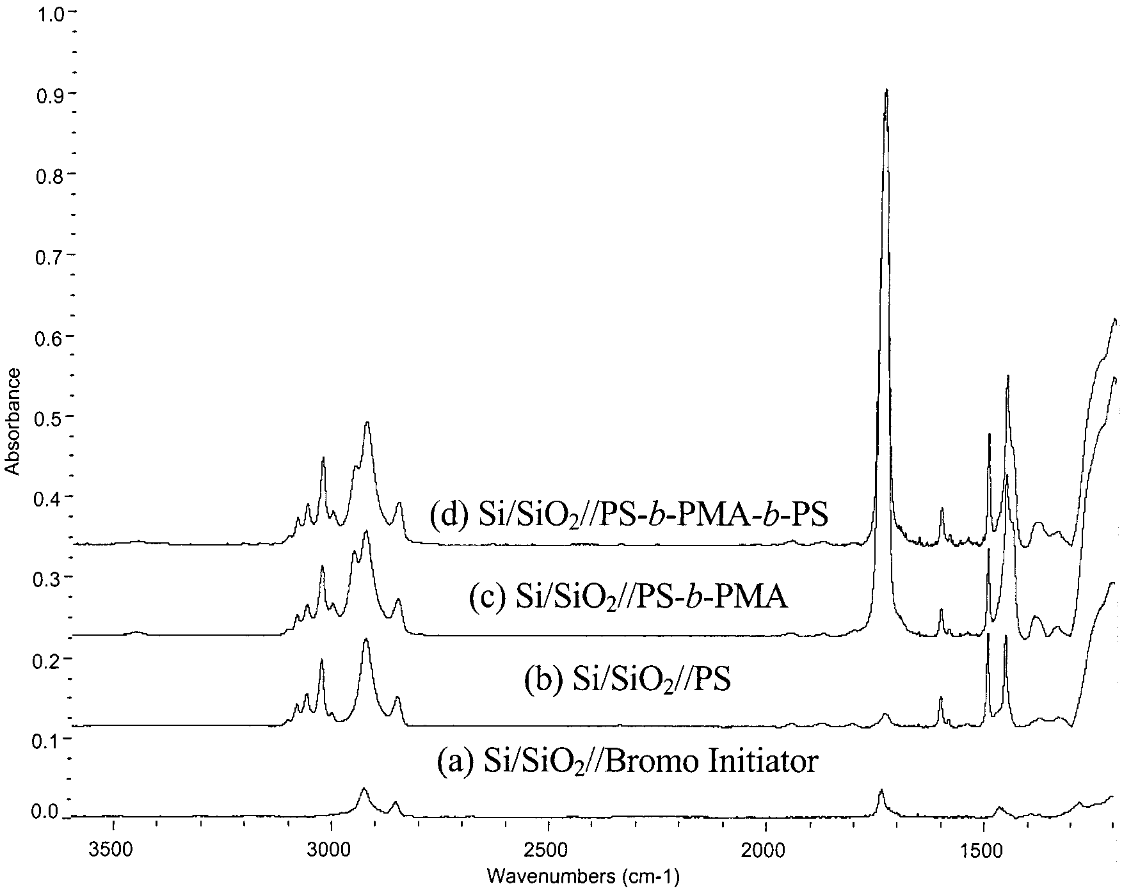

Figure 2. ATR−FTIR spectra of (a) Si/SiO$_2$//bromo-isobutyrate initiator, (b) Si/SiO$_2$//PS (tethered PS brush), (c) Si/SiO$_2$//PS-*b*-PMA, and (d) Si/SiO$_2$//PS-*b*-PMA-*b*-PS.

of the outer PMA layer to avoid contact with the nonsolvent may be difficult due to steric hindrance and thus results in a small amount of PMA remaining at the air interface.

To further analyze the composition of the triblock copolymer brushes at the air interface after solvent treatment, XPS was used. The sampling depth of the XPS experiments is approximately 5−10 nm, depending on the core level binding energy and takeoff angle.[31] Figure 3 shows the XPS spectra of the Si/SiO$_2$//PMA-*b*-PS-*b*-PMA triblock copolymer brush after treatment with CH$_2$Cl$_2$ (Figure 3a) and cyclohexane (Figure 3b). The molar contents of carbon and oxygen atoms after treatment with CH$_2$Cl$_2$ were 78.8 and 20.3%, respectively. After treatment with cyclohexane, the oxygen content decreased to 10.3% and the carbon content increased to 89.2%. In each case a small amount, approximately 0.5%, of silicon could be detected. For the Si/SiO$_2$//PS-*b*-PMA-*b*-PS triblock copolymer brush, the molar contents of carbon and oxygen atoms after treatment with CH$_2$Cl$_2$ were 85.4 and 14.1%, respectively. After treatment with acetone, the oxygen content increased to 17.3% and the carbon content decreased to 82.2%. Again, approximately 0.5% of silicon was detected in each case.

The XPS results confirm the observed water contact angle data of the composition of the triblock copolymer brushes at the air interface. The decrease in oxygen content of the Si/SiO$_2$//PMA-*b*-PS-*b*-PMA triblock brush, after treatment with cyclohexane, is consistent with the migration of the PMA blocks away from the air interface. However, as the oxygen content after cyclohexane treatment is still 10.3%, a significant amount of PMA is still at or close to the air interface, and as a result, the water contact angle is below the characteristic value of PS. Whereas, with the Si/SiO$_2$//PS-*b*-PMA-*b*-PS triblock brush the oxygen content increases after treatment with acetone, as the PS blocks migrate away from the air interface. The high oxygen content of the Si/SiO$_2$//PS-*b*-PMA-*b*-PS brush after treatment with CH$_2$Cl$_2$ is believed to be due to a combination of the thin outer PS layer and incomplete reinitiation of the middle PMA block. This results in an observed water contact angle significantly lower than the characteristic value for PS.

AFM of Tethered Triblock Copolymer Brushes. The AFM study of tethered Si/SiO$_2$//PS-*b*-poly(methyl methacrylate) (PMMA) and Si/SiO$_2$//PS-*b*-PMA brushes has been previously reported.[7] In this earlier work we reported the formation of a nanopattern from tethered Si/SiO$_2$//PS-*b*-PMMA and Si/SiO$_2$//PS-*b*-PMA brushes after treatment with block-selective solvents. This nanopattern was attributed to the formation of pinned micelles with the more soluble PS block migrating to the air interface as the less soluble PMMA or PMA block migrated to avoid contact with the solvent. We have used AFM to examine the effect of solvent treatment on the tethered triblock copolymer brushes in this study.

Figure 4 shows the tapping mode AFM images of the Si/SiO$_2$//PMA-*b*-PS-*b*-PMA brush after treatment with CH$_2$Cl$_2$ (Figure 4a) and cyclohexane (Figure 4b). Treatment with CH$_2$Cl$_2$ resulted in a relatively smooth featureless surface, with a surface roughness of 0.5 nm, where roughness is defined as the root-mean-square of

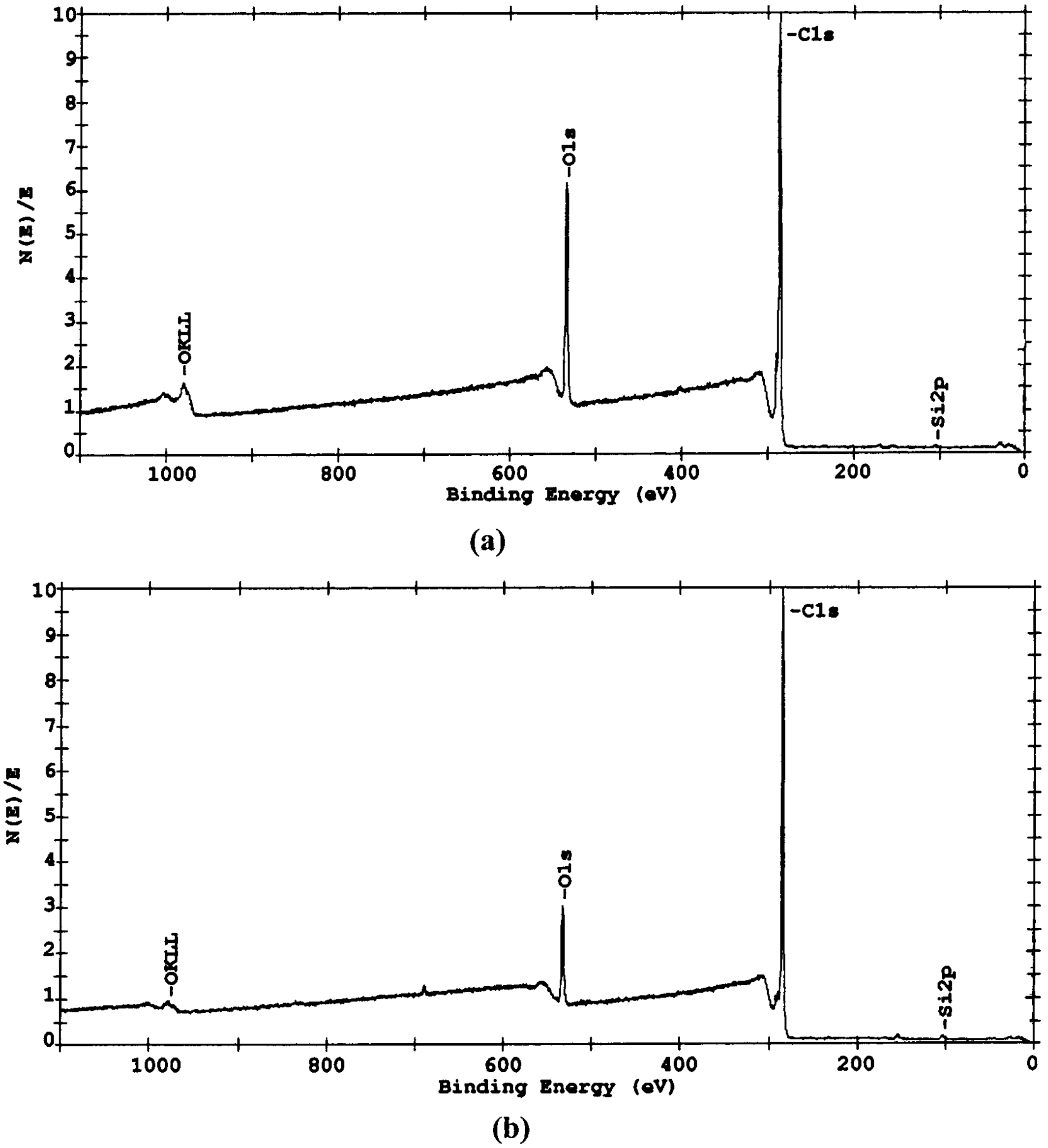

Figure 3. XPS spectra of tethered Si/SiO$_2$//PMA-*b*-PS-*b*-PMA brush (a) after treatment with CH$_2$Cl$_2$ and (b) after treatment with cyclohexane.

height deviations taken from the mean data plane. After treatment with cyclohexane, the surface roughness increased to 1.5 nm, and the sample exhibited an unusual nanomorphology. The average domain diameter of the nanomorphology, as determined by AFM, was 30 nm. Similar results were observed for the treatment of the Si/SiO$_2$//PS-*b*-PMA-*b*-PS brush with CH$_2$Cl$_2$ (Figure 5a) and acetone (Figure 5b). In this case the surface roughness of the CH$_2$Cl$_2$-treated sample was 0.8 nm, which increased to a roughness of 2.2 nm after treatment with acetone, and the average domain diameter was 20 nm.

For both triblock copolymer brushes, the formation of the nanomorphology after treatment with a good solvent for the middle block was attributed to migration of the outer block to avoid contact with the nonsolvent. The proposed scheme for the response of tethered triblock copolymer brushes to treatment with different solvent is shown in Scheme 2. For example, with the tethered Si/SiO$_2$//PMA-*b*-PS-*b*-PMA brush, CH$_2$Cl$_2$ is a good solvent for both PS and PMA. When the sample is immersed in this solvent, the polymer chains are forced to stretch away from the interface to avoid contact with the neighboring polymer chains. Removing the Si/SiO$_2$//PMA-*b*-PS-*b*-PMA brush from CH$_2$Cl$_2$ condenses the polymer brushes and localizes the outer PMA block at the air interface. If the sample is then immersed in cyclohexane at 40 °C, a good solvent for PS only, we speculate that the outer PMA segments migrate from the solvent interface and form aggregates with both neighboring PMA segments and PMA segments tethered to the surface, to avoid contact with the solvent. As the middle PS block is miscible with the cyclohexane, it migrates to the solvent interface to form a shield around the PMA aggregates. It should be noted that Scheme 2 is an idealized representation of the proposed switching mechanism and may be affected by other factors.

Comparison of the water contact angle, XPS, and AFM results indicates that the proposed rearrangement scheme may be influenced by a number of factors. These include the thickness of the outer block, the proximity of the tethered chains to each other, and the Flory–Huggins interaction parameter between PS and PMA. As can be seen in Figure 5a, treatment of the tethered Si/SiO$_2$//PS-*b*-PMA-*b*-PS brush with CH$_2$Cl$_2$ results in

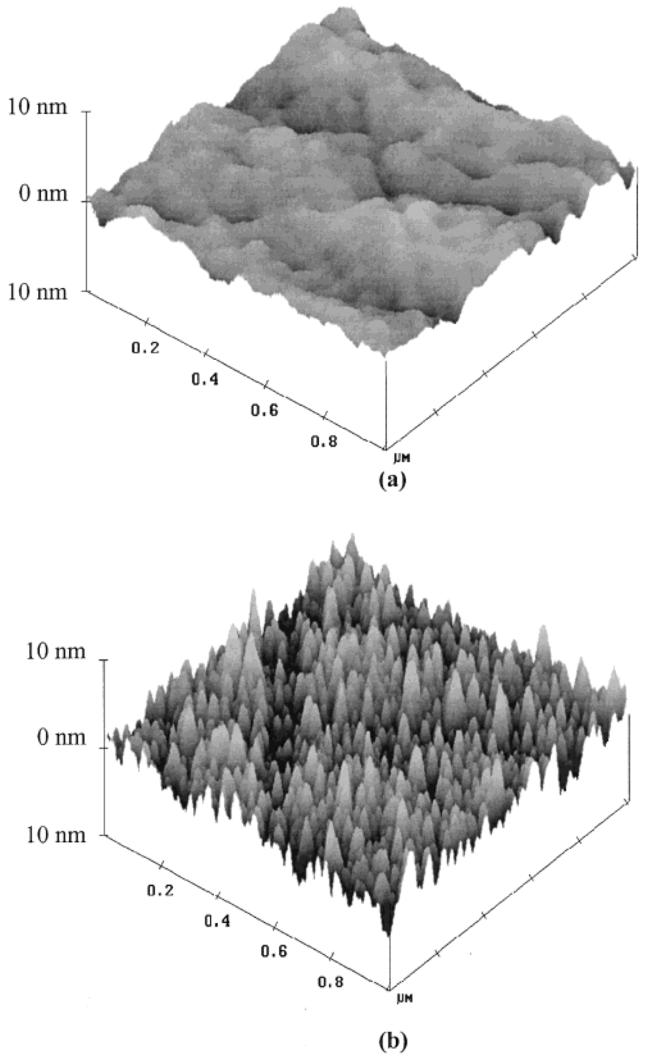

Figure 4. AFM images of Si/SiO$_2$//PMA-*b*-PS-*b*-PMA brush (a) after treatment with CH$_2$Cl$_2$ and (b) after treatment with cyclohexane.

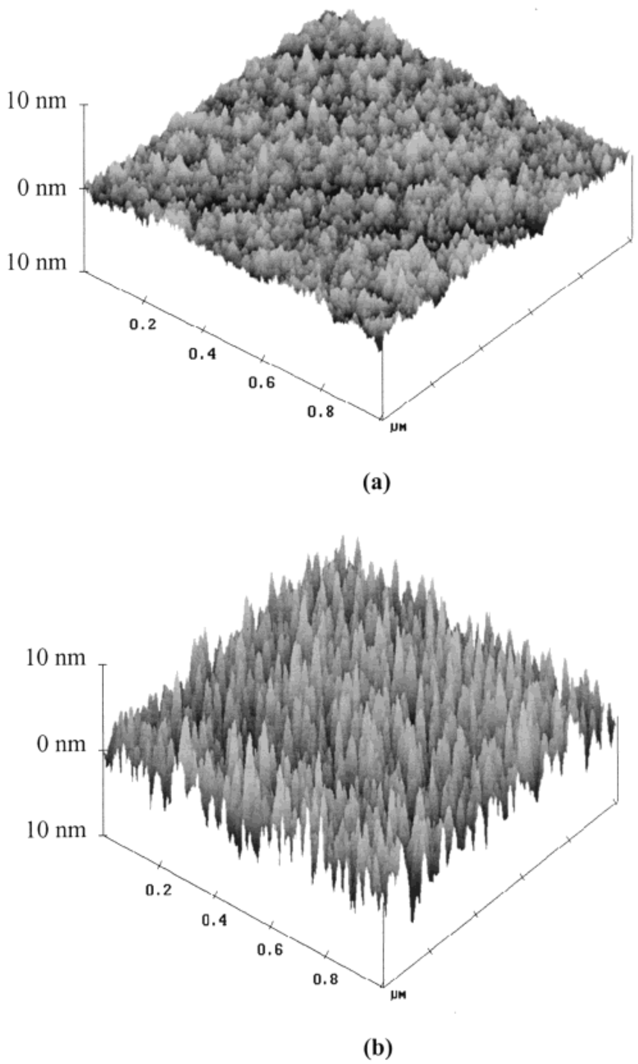

Figure 5. AFM images of Si/SiO$_2$//PS-*b*-PMA-*b*-PS brush (a) after treatment with CH$_2$Cl$_2$ and (b) after treatment with acetone.

a surface that is not smooth and featureless, as was obtained with the Si/SiO$_2$//PMA-*b*-PS-*b*-PMA brush. The Si/SiO$_2$//PS-*b*-PMA-*b*-PS brush had an outer PS layer thickness of only 3 nm, which was significantly smaller than the outer PMA layer in the Si/SiO$_2$//PMA-*b*-PS-*b*-PMA brush, which was 15 nm. The thin outer PS layer is believed to be responsible for the lower than expected water contact angle exhibited by the brush after treatment with CH$_2$Cl$_2$ and also for the relatively high oxygen content as measured by XPS. The "textured" surface seen in Figure 5a is believed to also contribute to these results and may arise due to the Flory−Huggins interaction parameter between PS and PMA. It has been previously reported[7] that the large Flory−Huggins interaction parameter between PS and PMA may give rise to phase separation not only in the vertical direction but also in the lateral direction. In our case, the thin and possibly incomplete (due to poor reinitiation of the middle MA block) outer PS layer may result in aggregation of the PS and thus expose the air interface to the underlying PMA.

The length of the outer block and proximity of the chains to each other may also play an important role in the formation of the observed nanomorphology after treatment with solvent. It has been previously reported[3,7] that solvent treatment of tethered diblock copolymer brushes where the more soluble block is attached to the surface and that the size of the resulting pinned-micelle morphology increases with the size of the less soluble block. A similar result was observed in our case, as the average domain size of the Si/SiO$_2$//PS-*b*-PMA-*b*-PS brush was 30 nm. For the Si/SiO$_2$//PMA-*b*-PS-*b*-PMA brush, the average domain size was 20 nm, and the length of the less soluble outer block was only 3 nm (compared to a 15 nm outer block length for the Si/SiO$_2$//PS-*b*-PMA-*b*-PS system). Previous work using a similar immobilized bromo-isobutyrate initiator indicated that deposition of the initiator using a solution method resulted in monolayers that were not completely uniform.[9] This, together with a potential decrease in reinitiation efficiency when using sequential ATRP polymerizations, may suggest in our case that the grafting density is too low to facilitate block mobility during the reorganization process.

Conclusions

Tethered triblock copolymer brushes of styrene and methyl acrylate were synthesized using sequential ATRP from self-assembled monolayer of a bromo-isobutyrate initiator. The Si/SiO$_2$//PS-*b*-PMA-*b*-PS and Si/SiO$_2$//PMA-*b*-PS-*b*-PMA brushes were characterized

Scheme 2. Proposed Responses of Tethered Triblock Copolymer Brushes to Different Solvent Treatments

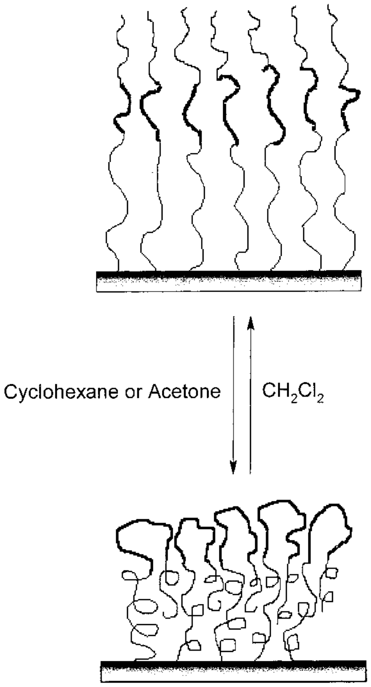

using ATR−FTIR, goniometry, and ellipsometry. The free polymer was analyzed by GPC. Upon treatment with different solvents, the tethered triblock copolymer brushes exhibited reversible changes in surface properties, which were monitored using goniometry and XPS analysis. AFM analysis of the treated brushes indicated that unusual nanomorphologies were formed when treated with a solvent that was a good solvent for the middle block but a nonsolvent for the tethered and outer blocks. We believe that the observed nanomorphology is dependent on the thickness of the blocks, the proximity of the chains to each other, and the interaction parameter between the different components.

Acknowledgment. This work was supported by the National Science Foundation (DMR-0072977). We thank Dr. W. Jennings for assistance with XPS.

References and Notes

(1) Milner, S. T. *Science* **1991**, *251*, 905.
(2) Halpern, A.; Tirrell, M.; Lodge, T. P. *Adv. Polym. Sci.* **1992**, *100*, 31.
(3) Zhulina, E. B.; Singh, C.; Balazs, A. C. *Macromolecules* **1996**, *29*, 6338.
(4) Zhulina, E. B.; Singh, C.; Balazs, A. C. *Macromolecules* **1996**, *29*, 8254.
(5) Ito, Y.; Nishi, S.; Park, Y. S.; Imanishi, Y. *Macromolecules* **1997**, *30*, 5856.
(6) Park, Y. S.; Ito, Y.; Imanishi, Y. *Macromolecules* **1998**, *31*, 2606.
(7) Zhao, B.; Brittain, W. J.; Zhou, W.; Cheng, S. Z. D. *Macromolecules* **2000**, *33*, 8821.
(8) Zhao, B.; Brittain, W. J.; Zhou, W.; Cheng, S. Z. D. *J. Am. Chem. Soc.* **2000**, *122*, 2407.
(9) Kong, X.; Kawai, T.; Abe, J.; Iyoda, T. *Macromolecules* **2001**, *34*, 1837.
(10) Mayes, A. M.; Kumar, S. K. *MRS Bull.* **1997**, *22* (1), 43.
(11) Belder, G. F.; ten Brinke, G.; Hadziioannou, G. *Langmuir* **1997**, *13*, 4102.
(12) Mansky, P.; Liu, Y.; Huang, E.; Russell, T. P.; Hawker, C. *Science* **1997**, *275*, 1458.
(13) Zhao, B.; Brittain, W. J. *Prog. Polym. Sci.* **2000**, *25*, 677.
(14) Ito, Y.; Ochiai, Y.; Park, Y. S.; Imanishi, Y. *J. Am. Chem. Soc.* **1997**, *119*, 1619.
(15) Prucker, O.; Rühe, J. *Macromolecules* **1998**, *31*, 592.
(16) Prucker, O.; Rühe, J. *Macromolecules* **1998**, *31*, 602.
(17) Matyjaszewski, K. In *Controlled/Living Radical Polymerization*; Matyjaszewski, K., Ed.; ACS Symposium Series 768; American Chemical Society: Washington, DC, 2000; p 2.
(18) Husseman, M.; Malmstrom, E. E.; McNamara, M.; Mate, M.; Mecerreyes, O.; Benoit, D. G.; Hedrick, J. L.; Mansky, P.; Huang, E.; Russell, T. P.; Hawker, C. J. *Macromolecules* **1999**, *32*, 1424.
(19) Matyjaszewski, K.; Miller, P. J.; Shukla, N.; Immaraporn, B.; Gelman, A.; Luokala, B. B.; Siclovan, T. M.; Kickelbick, G.; Vallant, T.; Hoffmann, H.; Pakula, T. *Macromolecules* **1999**, *32*, 8716.
(20) Ejaz, M.; Yamamoto, S.; Ohno, K.; Tsujii, Y.; Fukuda, T. *Macromolecules* **1998**, *31*, 5934.
(21) Böttcher, H.; Hallensleben, M. L.; Nuâ, S.; Wurm, H. *Polym. Bull. (Berlin)* **2000**, *44*, 223.
(22) Ejaz, M.; Ohno, K.; Tsujii, Y.; Fukuda, T. *Macromolecules* **2000**, *33*, 2870.
(23) Kong, X.; Kawai, T.; Abe, J.; Iyoda, T. *Macromolecules* **2001**, *34*, 1837.
(24) Keller, R. N.; Wycoff, H. D. *Inorg. Synth.* **1946**, *2*, 1.
(25) *Polymer Handbook*; Brandrup, J., Immergut, E. H., Grulke, E. A., Eds.; Wiley & Sons: New York, 1999.
(26) Ejaz, M.; Tsujii, Y.; Fukuda, T. *Polymer* **2001**, *42*, 6811.
(27) Tsujii, Y.; Ejaz, M.; Sato, K.; Goto, A.; Fukuda, T. *Macromolecules* **2001**, *34*, 8872.
(28) Extrand, C. W.; Kumagai, Y. *J. Colloid Interface Sci.* **1997**, *191*, 378.
(29) Davis, K. A.; Matyjaszewski, K. *Macromolecules* **2000**, *33*, 4039.
(30) Davis, K. A.; Matyjaszewski, K. *Macromolecules* **2001**, *34*, 2101.
(31) Zhao, B.; Brittain, W. J. *Macromolecules* **2000**, *33*, 8813.

MA020109M